GLIA 55:1169–1177 (2007)

Distinct Regulation of MHC Molecule Expression on Astrocytes and Microglia During Viral Encephalomyelitis

LUDWIG HAMO,[1] STEPHEN A. STOHLMAN,[1,2,3] MAYA OTTO-DUESSEL,[3] AND CORNELIA C. BERGMANN[2]*
[1]*Department of Neuroscience, University of Southern California Keck School of Medicine, Los Angeles, California*
[2]*Department of Neurology, University of Southern California Keck School of Medicine, Los Angeles, California*
[3]*Department of Molecular Microbiology and Immunology, University of Southern California Keck School of Medicine, Los Angeles, California*

KEY WORDS
astrocytes; glia; coronavirus; antigen presentation; MHC

ABSTRACT
The potential interplay of glial cells with T cells during viral induced inflammation was assessed by comparing major histocompatibility complex molecule upregulation and retention on astrocytes and microglia. Transgenic mice expressing green fluorescent protein under control of the astrocyte-specific glial fibrillary acidic protein promoter were infected with a neurotropic coronavirus to facilitate phenotypic characterization of astrocytes and microglia using flow cytometry. Astrocytes in the adult central nervous system up-regulated class I surface expression, albeit delayed compared with microglia. Class II was barely detectable on astrocytes, in contrast to potent up-regulation on microglia. Maximal MHC expression in both glial cell types correlated with IFN-γ levels and lymphocyte accumulation. Despite a decline of IFN-γ concomitant to virus clearance, MHC molecule expression on glia was sustained. These data demonstrate distinct regulation of both class I and class II expression by microglia and astrocytes *in vivo* following viral induced inflammation. Furthermore, prolonged MHC expression subsequent to viral clearance implies a potential for ongoing presentation.

INTRODUCTION

MHC molecules, required for T cell activation and effector recognition, are not constitutively expressed on central nervous system (CNS) resident cells (Aloisi et al., 2000; Sedgwick and Hickey, 1997; Xiao and Link, 1998). Restrictions on T cell surveillance are further imposed by the blood brain barrier and absence of classical lymphatic drainage (Aloisi et al., 2000; Hickey, 2001; Xiao and Link, 1998). This quiescent state is rapidly overcome following CNS infections. During virus induced inflammation, microglia readily up-regulate both class I and class II MHC molecules in the presence of IFN-γ secreted by T cells (Bergmann et al., 2003). However, *in vivo* detection of MHC molecules on astrocytes and oligodendrocytes during inflammation has been more difficult (Horwitz et al, 1999; Redwine et al., 2001; Stuve et al., 2002; Traugott et al., 1985). Whereas class I expression was detected on oligodendroglia during a neuronotropic viral infection, it was not detected on astrocytes (Redwine et al., 2001). Nevertheless, infection of cultured astrocytes with mouse hepatitis virus (MHV) induces MHC up-regulation (Gilmore et al., 1994; Lavi et al., 1989; Suzumura et al., 1986). Furthermore, although IFN-γ readily increases constitutive MHC class I expression and induces class II expression on cultured astrocytes derived from neonates (Fierz et al., 1985; Massa et al., 1993; Wong et al., 1985), constitutive transgenic IFN-γ expression was unable to induce class I or class II expression on astrocytes *in vivo* (Horwitz et al., 1999). Systemic administration of IFN-γ to mice also did not induce class II expression on astrocytes (Momburg et al., 1986), whereas intracerebral injection did (Wong et al., 1984). The recent unequivocal demonstration of class I expression on astrocytes *in vivo* following CNS adenoviral infection by confocal microscopy (Barcia et al., 2006), in addition to indirect evidence for MHC restricted $CD8^+$ T cell function (Cabarrocas et al., 2003; Lin et al., 1997) suggests technical limits imposed by histological analysis (Lampson, 1995) may have underestimated MHC expression.

In contrast to the $CD45^{lo}$ phenotype used to identify microglia, identification of astrocytes derived from the adult CNS has been hampered by the lack of a suitable surface marker. This study takes advantage of transgenic mice expressing the green fluorescent protein (GFP) under control of the astrocyte-specific glial fibrillary acidic protein (GFAP) promoter (Zhuo et al., 1997) to directly analyze surface molecule expression on GFP^+ astrocytes derived from the adult inflamed CNS by flow cytometry. Encephalomyelitis was induced by infection with a neurotropic coronavirus variant designated JHMV. Infection of adult mice induces an immune-mediated primary demyelination, and has served as a model for the human demyelinating disease, multiple sclerosis (Bergmann et al., 2006). JHMV infection induces encephalitis in most strains of mice, infecting ependymal cells,

Grant sponsor: US National Institutes of Health; Grant numbers: NS18146, NS40667, AI47249.

Stephen A. Stohlman is currently at Department of Neurosciences, Lerner Research Institute, The Cleveland Clinic, Cleveland, OH 44195.

Maya Otto-Duessel is currently at Department of Radiology, Saban Research Institute of Childrens Hospital Los Angeles, Los Angeles, CA 90027.

*Correspondence to (current address): Cornelia Bergmann; Department of Neurosciences, Lerner Research Institute, The Cleveland Clinic, 2500 Euclid Avenue, NC30, Cleveland, OH 44195. E-mail: bergmac@ccf.org

Received 22 December 2006; Revised 17 May 2007; Accepted 4 June 2007

DOI 10.1002/glia.20538

Published online 28 June 2007 in Wiley InterScience (www.interscience.wiley.com).

microglia, astrocytes, and oligodendrocytes, but rarely neurons (Wang et al., 1992). Following a vigorous CNS inflammatory response, infectious virus is generally cleared by $CD8^+$ T cells within 2 weeks of infection (Bergmann et al., 2006). Control of virus infection in microglia and astrocytes is dependent on perforin-mediated cytolysis (Lin et al., 1997), implicating class I antigen presentation to virus-specific $CD8^+$ T cells. By contrast, viral clearance from oligodendrocytes appears independent of perforin-mediated cytolysis, but requires IFN-γ (Bergmann et al., 2003; Parra et al., 1999). Despite control of infectious virus by two anti-viral effector mechanisms, viral antigen and RNA persists in the absence of detectable infectious virus (Bergmann et al., 2006). Viral persistence appears to be restricted to astrocytes (Perlman and Ries, 1987) and oligodendrocytes (Lavi et al., 1984; Parra et al., 1999; Ramakrishna et al., 2003). Loss of CD8 T cell effector function as well as poor MHC expression on glial subsets potentially contributes to the inability of T cells to control viral persistence (Ramakrishna et al., 2006).

MHC molecule expression on astrocytes was compared with microglia during viral encephalomyelitis in adult mice using flow cytometry. Astrocytes strongly up-regulated class I, albeit delayed compared with microglia. By contrast, class II remained undetectable on the majority of astrocytes, differing from the potent class II up-regulation on microglia. However, once induced, MHC molecule surface expression was maintained following virus clearance and down regulation of IFN-γ. These novel data highlight the distinct abilities of microglia and astrocytes to up-regulate expression of class I and class II molecules in response to virus-induced inflammation and suggest that prolonged MHC expression may provide an opportunity for auto antigen presentation.

MATERIALS AND METHODS

Mice, Viruses, and Virus Titration

Mice expressing GFP under control of the human GFAP promoter (FVB/N-Tg[GFAPGFP]14Mes/J) (Zhuo et al., 1997) were purchased from The Jackson Laboratory (Bar Harbor, ME) and bred in an accredited animal facility at the Keck School of Medicine, University of Southern California, Los Angeles, CA. All procedures were carried out in compliance with Institutional Animal Care and Use Committee approved protocols. Six- to seven-week-old mice of both sexes were injected in the left cerebral hemisphere (i.c.) with 30 μL of endotoxin-free PBS containing 500 plaque forming units (PFU) of the 2.2-v1 mAb-derived variant of JHMV (Fleming et al., 1986). Clinical symptoms were evaluated daily based on a 0–4 scale as previously described (Fleming et al., 1986). Briefly, mice were graded as: 0 = healthy; 1 = ruffled hair and hunchbacked appearance; 2 = reduced mobility and inability to upright; 3 = paralysis and wasting; 4 = death. To determine virus replication within the CNS one half brains from individual mice were homogenized in 4 mL sterile phosphate buffer saline (pH 7.4) using ice cold Tenbroeck tissue homogenizers. Homogenates were centrifuged at 500*g* for 7 min at 4°C. Supernatants were frozen at −70°C for determination of infectious virus by plaque assay carried out on monolayers of the DBT astrocytoma cell line as previously described (Fleming et al., 1986; Lin et al., 1997).

Isolation of CNS Derived Cells

For isolation of $CD45^{hi}$ bone marrow derived CNS infiltrating cells, pooled brains (n = 3–4 per time point) were homogenized and centrifuged at 500*g* for 7 min at 4°C as described earlier for virus supernatants. Cell pellets were resuspended in PBS and adjusted to 30% Percoll (Pharmacia, Uppsala, Sweden). Following addition of a 1 mL 70% Percoll underlay and centrifugation at 800*g* at 4°C for 25 min cells were isolated from the 30%/70% interface, washed in RPMI medium, and resuspended in PBS containing 0.5% BSA. Astrocytes were isolated using proteolytic digestion as previously described for oligodendrocytes (Gonzales et al., 2005). Brains from 3 to 4 mice per time point were combined, rinsed in RPMI supplemented with 25 mM HEPES (pH 7.2) and 1% fetal calf serum (FCS), and placed into 100 mm plates. After finely mincing in 1 mL RPMI supplemented with HEPES and 1% fetal FCS with razor blades, 4 mL of a prewarmed 0.25% trypsin solution was added per brain, and digestions carried out in 50 mL tubes at 37°C for 30 min with intermittent agitation. Digestion was terminated by addition of 5 mL of ice cold RPMI containing 20% FCS per brain. Following centrifugation at 500*g* for 7 min at 4°C, cells were resuspended in RPMI supplemented with 25 mM HEPES containing 30% Percol, and concentrated by centrifugation onto a 70% Percol cushion as described earlier.

Mixed Glial Cell Cultures

Brains were isolated from newborn FVB/N-Tg-[GFAPGFP]14Mes/J mice and glial cells cultured as described (Hindinger et al., 2005). After removal of meninges and superficial blood vessels frontal lobes were digested with 0.25% trypsin in PBS containing 0.02% EDTA for 20 min at 37°C and dissociated by trituration. Cells from 3 to 5 mice were added to 75 cm T flasks containing Dulbecco's modified minimal essential medium (Irvine Scientific, Santa Ana, CA) supplemented with 10% FCS and penicillin (1000 units/mL)/streptomycin (1000 μg/mL). Medium was replaced after 12–16 h at 37°C and subsequently at 3 day intervals. Cells were subcultured once after 7–10 days and used at confluency. Mixed glial cultures were incubated in the presence or absence of 1 ng/mL recombinant murine IFN-γ (BD PharMingen, San Diego, CA) for 48 h. MHC class I and class II expression was analyzed following trypsinization (0.025% trypsin/EDTA) of monolayers by flow cytometry.

Flow Cytometry

CNS derived cells were incubated at 4°C for 20 min with anti-FcIII/IIR mAb (2.4G2) (BD PharMingen) and

2% mouse serum to block nonspecific binding. Surface expression was determined using mAb for CD4 (clone GK1.5), CD8 (53-6.7), CD11b (M1/70), CD45 (30-F11), NK1.1 (PK135), MHC class II (M5-114) (all from BD PharMingen), MHC class I (mAb 28-14-8) (eBiosciences, San Diego, CA), and F4/80 (A3-1, Serotec, Raleigh, NC) conjugated with APC, PE, or PerCP. Isotype control mAb for class I and class II were mouse IgG_{2a} (mAb 28-14-8) (eBiosciences, San Diego, CA) and rat IgG_{2b},κ (BD PharMingen), respectively. Cells were incubated with Ab for 30 min at 4°C and washed twice before analysis on a FACSCalibur flow cytometer (Becton Dickinson, Mountain View, CA). Astrocytes were defined as GFP^+CD45^- cells, microglia as $CD45^{lo}$ cells, and infiltrating cells as $CD45^{hi}$. Data were analyzed using CellQuest-Pro (Becton Dickinson) or Flowjo software (Tree Star, Ashland, OR).

IFN-γ Detection

IFN-γ was measured in supernatants from brain homogenates of infected mice by ELISA. Supernatants were prepared in PBS as described earlier and stored at −70°C. Briefly, 96-well plates coated overnight with 100 ng of IFN-γ mAb (R4-6A2) in carbonate buffer (0.1 M, pH 9.5) at 4°C were washed 3 times with PBS containing 0.05% Tween 20 (Sigma) and blocked with PBS containing 10% FCS for 1 h at RT. Serial twofold diluted brain supernatants or IFN-γ standard (BD PharMingen) were added in duplicate. Samples were incubated at RT for 2 h, and washed prior to addition of biotinylated anti-IFN-γ mAb (XMG1.2) and avidin-horseradish peroxidase. Color was developed following addition of tetramethylbenzidine Reagent (BD PharMingen) and absorbance measured at 405 nm using a Microplate Autoreader model 680, with data analyzed using Microplate Manager 5.2 software (Bio-Rad, Hercules, CA).

Histology

Brains and spinal cords were examined for inflammation, demyelination, and distribution of viral Ag. Tissues were fixed for 3 h in Clark's solution (75% ethanol, 25% glacial acetic acid) prior to embedding. Sections were stained with hematoxylin and eosin (H&E) to determine inflammation and luxol fast blue (LFB) to determine demyelination. Distribution of viral Ag was determined by immunoperoxidase staining (Vectastain-ABC kit; Vector Laboratory, Burlingame, CA) using the anti-JHMV mAb J.3.3 specific for the carboxyl terminus of the viral nucleocapsid protein as the primary Ab and horse anti-mouse as secondary Ab (Vector Laboratory). Sections were scored for inflammation, demyelination, and viral Ag in a blinded fashion. Representative fields were identified based on average scores of all sections in each experimental group.

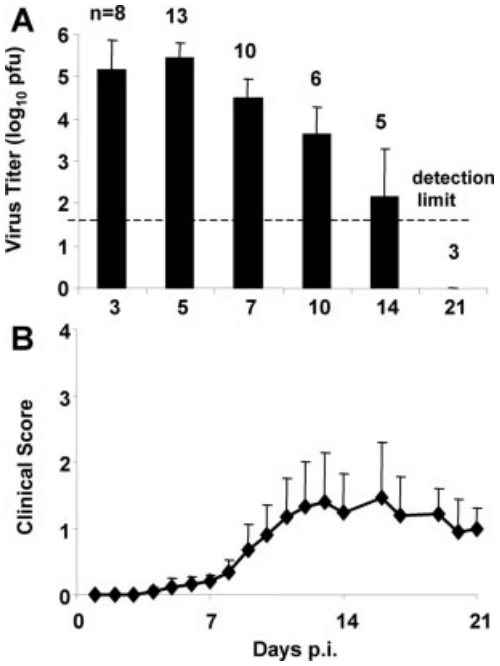

Fig. 1. JHMV Pathogenesis of in FVB/N GFAP-GFP mice. **(A)** Virus titers in brains of individual mice expressed as pfu/gram tissue. Numbers above bars indicate mice at each time point; error bars represent standard deviation. **(B)** Clinical disease induced by JHMV infection. Data are the average of 5 experiments.

RESULTS

JMHV Pathogenesis In GFAP-GFP Transgenic Mice

JHMV infection elicits an acute encephalomyelitis, accompanied by demyelination that resolves into a chronic demyelinating disease characterized by persistence of viral antigen and RNA in BALB/c ($H\text{-}2^d$) and C57BL/6 ($H\text{-}2^b$) mice (Bergmann et al., 2006). To confirm susceptibility and similar pathogenesis in FVB/N ($H\text{-}2^q$) mice expressing GFP in astrocytes, virus replication within the CNS and clinical symptoms were monitored until 21 days post infection (p.i.) (see Fig. 1). Virus replication in the CNS of infected transgenic FVB/N mice peaked at 5 days p.i. and then declined to undetectable levels in all mice by 21 days p.i. (Fig. 1A). These data are consistent with the kinetics of acute JHMV replication in the CNS of both $H\text{-}2^d$ and $H\text{-}2^b$ mice (Lin et al., 1997; Ramakrishna et al., 2002), with the exception of residual infectious virus at day 14 p.i., which is not observed in the latter strains. Clinical symptoms in infected FVB/N mice were observed as early as day 5 p.i., and all mice were symptomatic by day 10 p.i. (Fig. 1B). Clinical symptoms reached a plateau between days 13 and 18 p.i. and gradually declined thereafter, with the majority of mice exhibiting essentially complete clinical recovery (Fig. 1B). Although overall onset of symptoms was similar to BALB/c and C57BL/6 mice, the severity in infected FVB/N mice was reduced from an average score of ~2.5 (Lin

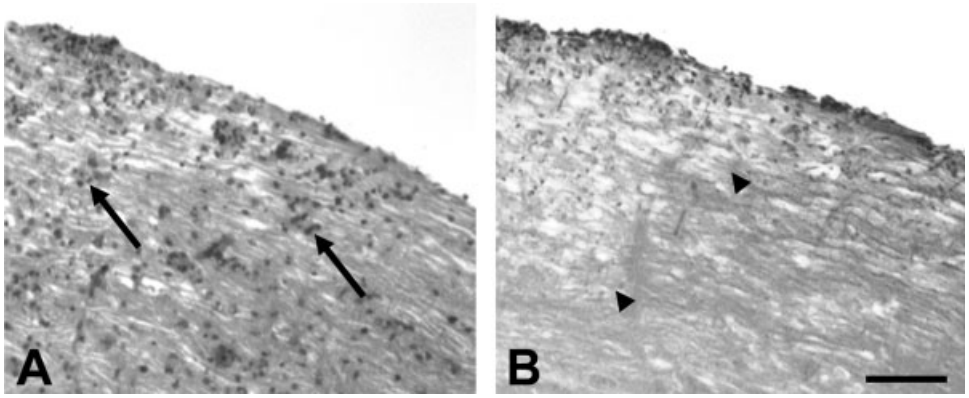

Fig. 2. Inflammation and demyelination in the CNS of JHMV infected FVB/N mice. Inflammation and demyelination in longitudinal sections of spinal cord from JHMV infected FVB/N mice at 10 days p.i. Mononuclear cell infiltration into both gray and white matter (panel **A**). H&E stain, arrows mark areas of mononuclear cell infiltration. Demyelination in a longitudinal spinal cord section (panel **B**). LFB stain, arrowheads mark areas of focal myelin loss. Bar = 400 μm.

et al., 1997; Parra et al., 1999; Ramakrishna et al., 2002) to ~1.5 in FVB/N mice. Despite the reduced clinical symptoms, JHMV infection induced a prominent inflammatory response in both brain (data not shown) and spinal cord (see Fig. 2), as well as vigorous demyelination predominantly in the spinal cord (see Fig. 2).

Cellular Infiltration into the CNS

The reduced clinical symptoms in FVB/N mice suggested the possibility that the inflammatory response differed from those characterized in other strains of infected mice. Therefore, the composition and kinetics of cells entering the CNS of the infected FVB/N mice were analyzed by flow cytometry. Infiltrating $CD45^{hi}$ cells peaked at 7 days p.i. (Fig. 3A), declined by day 10 p.i. and persisted out to day 21 p.i. Initial infiltrates comprised mainly innate components (Fig. 3B). Although macrophages dominated, neutrophils and NK cells were also recruited into the infected CNS. Neutrophils peaked early and rapidly disappeared by day 5 p.i., while infiltration of NK cells was maximal between days 5 and 7 p.i. and gradually decreased thereafter. As the number of total infiltrates increased, the percentage of the macrophages declined and T cells became prominent (Fig. 3C). While total T cells constituted $\sim 3 \times 10^5$ and 10×10^5 of the infiltrates at days 5 and 7, respectively, NK cells remained relatively constant at $\sim 2.5 \times 10^5$. $CD4^+$ T cells consistently outnumbered $CD8^+$ T cells by at least 2:1 throughout the course of infection. The increased ratio of $CD4^+$ T cells to $CD8^+$ T cells distinguishes the pathogenesis in FVB/N mice from both BALB/c and C57BL/6 mice, in which $CD8^+$ T cells prevail by day 8 p.i. Nevertheless, JHMV infection of FVB/N mice overall induces an acute encephalomyelitis closely resembling the pathogenesis in previously described mouse strains (Bergmann et al., 2006).

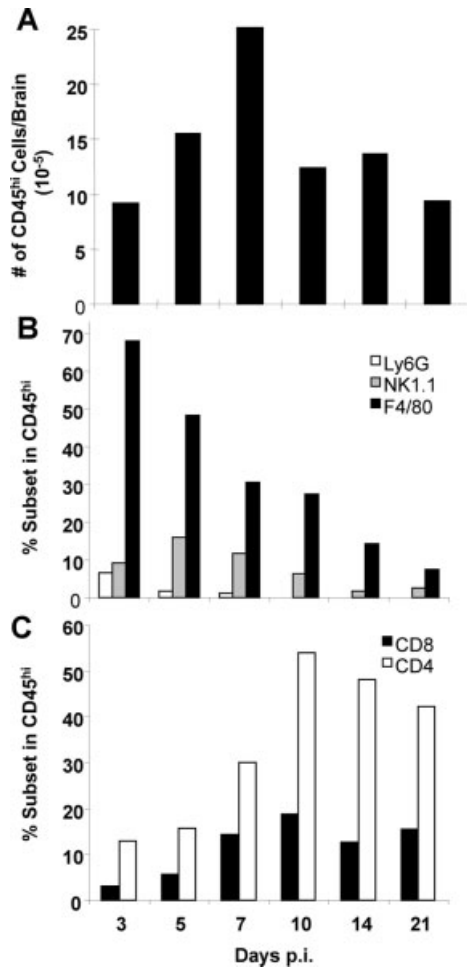

Fig. 3. Inflammatory response following JHMV infection. Infiltrating cell numbers identified by their $CD45^{hi}$ phenotype using flow cytometric analysis at indicated days p.i. (**A**). Cell subsets within the infiltrating cells identified as macrophages (F4/80), natural killer cells (NK1.1) and neutrophils (Ly-6G) (**B**), as well as $CD8^+$ and $CD4^+$ T cells (**C**). Data are from pooled mice (n = 3–4 per time point) and representative of 2–3 separate experiments.

In Vivo MHC Expression During Viral Induced Inflammation

JHMV infection induces both MHC class I and class II expression on microglia by 6 days p.i. and expression correlates with maximal T cell infiltration and IFN-γ secretion (Bergmann et al., 2003). Whereas expression of MHC class II on microglia is strictly IFN-γ dependent, class I is induced, albeit at lower levels and more transiently in the absence of IFN-γ (Bergmann et al., 2003). To compare regulation of MHC molecule expression on astrocytes to microglia by flow cytometry GFP^+ astrocytes were isolated from the adult CNS. Mechanical preparation of CNS derived cells, used to characterize $CD45^{hi}$ infiltrating cells and $CD45^{lo}$ microglia, did not yield appreciable GFP^+ glia. Therefore, a mild trypsin digestion was employed to release astrocytes from brain tissues as previously described for isolation of oligodendrocytes (Gonzalez et al., 2005; Ramakrishna et al., 2006). This approach typically resulted in 3–15% GFP^+ $CD45^-$ astrocytes within total viable cells recovered from the brains and was thus used to monitor MHC expression patterns on microglia and astrocytes throughout the course of JHMV infection (see Fig. 4).

Class I expression on $CD45^{lo}$ microglia was directly compared with class I^+ $CD45^{hi}$ cells (Fig. 4B) and increases in class I surface expression over time depicted relative to naïve microglia (Figs. 4B,C). Microglia from naïve mice exhibited low amounts of constitutive expression, as indicated by the shift in class I staining relative to isotype control. This baseline class I expression on microglia from naïve mice contrasts the inability to detect surface class I on microglia from naïve BALB/c or C57BL/6 mice (data not shown), but may reside in reactivity of the class I 28-14-8 mAb. A substantial population of microglia up-regulated MHC class I by day 3 p.i. (Fig. 4C). Expression levels increased further by day 5 p.i., reached maximal levels by day 7 p.i. and remained high out to 21 days p.i. Class I expression on microglia exceeded that of the majority of infiltrating cells by day 10 p.i. These data are consistent with upregulation of MHC class I expression on microglia derived from infected BALB/c mice (Bergmann et al., 2003). No MHC class I expression was detected on astrocytes derived from uninfected adult mice (Fig. 4D). Following infection up-regulation of MHC class I on astrocytes lagged compared with microglia. Although class I expression was barely detectable by day 3 p.i., (22% class I^+ astrocytes vs. 63% microglia), it gradually increased thereafter. By day 7 p.i. nearly 100% of astrocytes expressed class I and expression was maintained through 21 days p.i., similar to microglia.

To confirm the paucity of MHC class II expression by astrocytes *in vivo* (Horwitz et al., 1999; Redwine et al., 2001), class II expression on astrocytes was compared with microglia by flow cytometry. Neither microglia nor astrocytes from naïve mice expressed detectable levels of class II (Figs. 5A,B). Microglia revealed a defined population expressing class II by day 5 p.i., which increased prominently by day 7 p.i. (Fig. 5A). By day 10 p.i. all

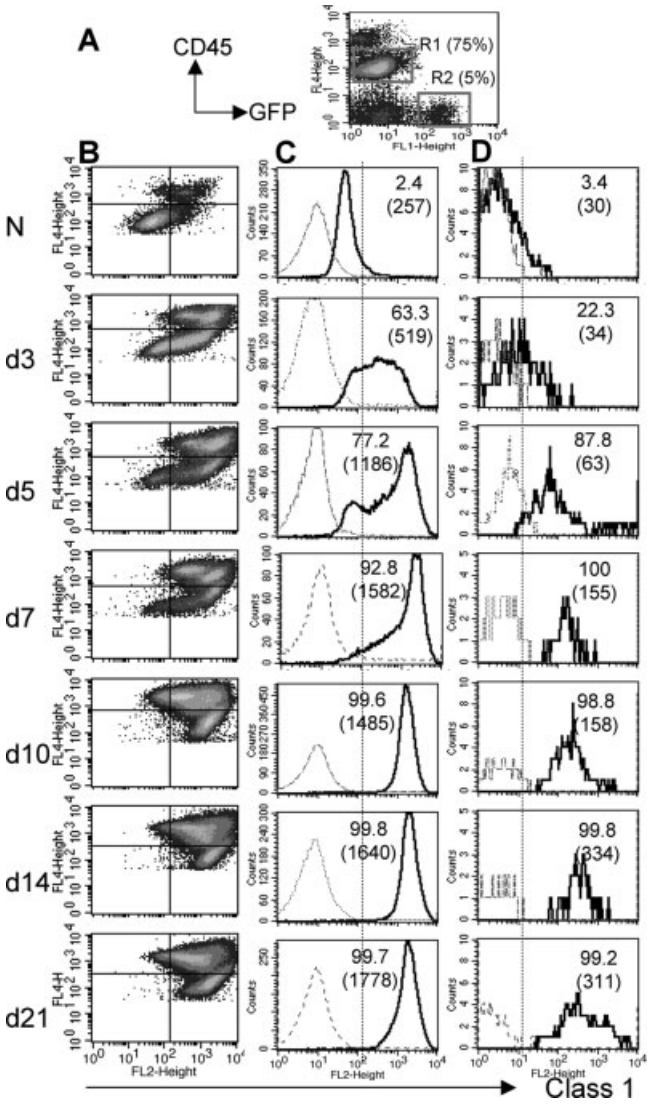

Fig. 4. Delayed MHC class I expression on astrocytes compared with microglia. CNS cells from naive (N) and infected mice analyzed for CD45 and MHC class I expression by flow cytometry at the indicated days p.i. (**A**) Representative density plot depicting $CD45^{lo}$ microglia in the R1 region and $CD45^-$ GFP^+ astrocytes in the R2 region from brains of naïve mice; numbers indicate percentages of cells in these gates. (**B**) Density plots showing class I expression on $CD45^{lo}$ microglia relative to $CD45^{hi}$ cells gated on total $CD45^+$ cells. Histograms show kinetics of class I expression on microglia (**C**; R1 gate) and astrocytes (**D**; R2 gate) indicated by solid black lines. Mouse IgG2a isotype control staining is indicated by thin dashed lines. Numbers within histograms represent percentage of glia with upregulated class I expression relative to naïve mice indicated by the dotted vertical line; numbers in brackets depict median fluorescent intensity (MFI) in the population with increased class I expression. Data are representative of 3–4 experiments.

microglia expressed high levels of class II and expression was sustained through day 21 p.i. By contrast, expression of MHC class II on astrocytes was tenuous (Fig. 5B). Although a slight shift in fluorescence was evident throughout days 7–21 p.i. on ~20% of astrocytes, the extent of class II expression was very low compared with microglia and limited to a small subset.

To confirm IFN-γ inducible MHC expression patterns observed in astrocyte cultures derived from other mouse

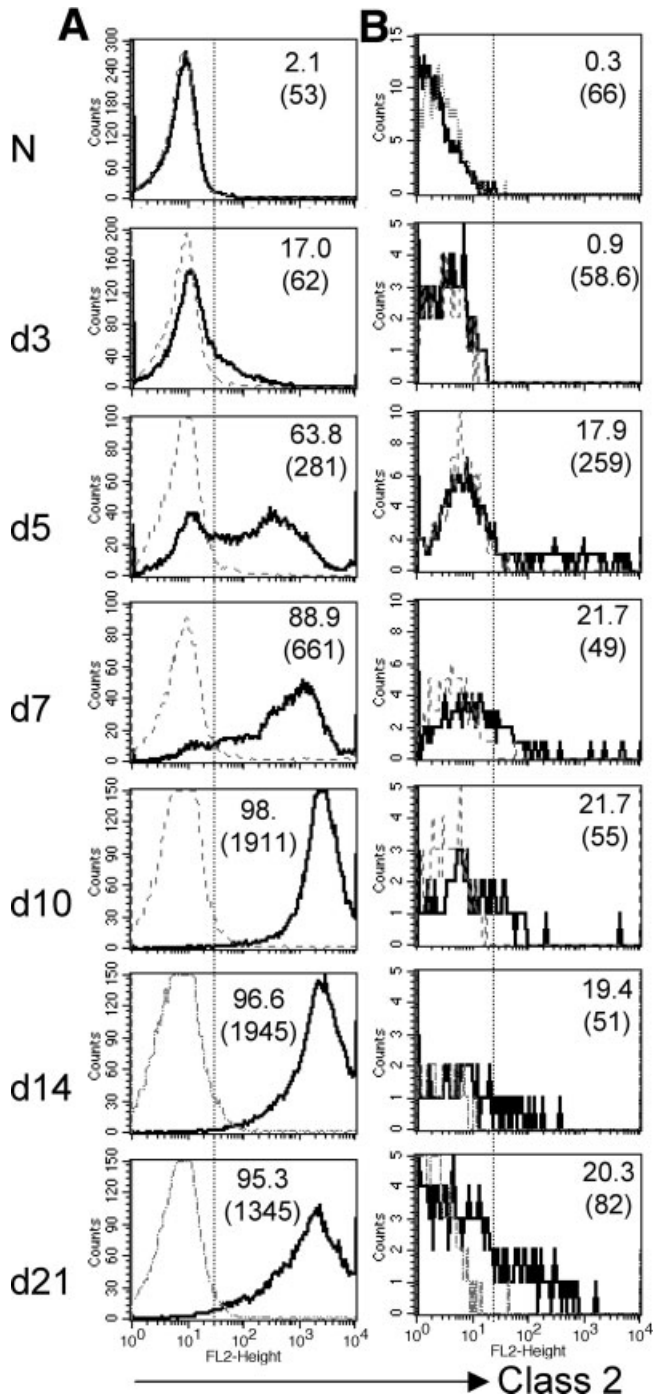

Fig. 5. MHC class II expression on microglia and astrocytes. CNS cells from uninfected and infected mice were analyzed for MHC class II expression on microglia and astrocytes as depicted in Fig. 4. Histograms show kinetics of class II expression on microglia (**A**; R1 gate) and astrocytes (**B**; R2 gate). Rat IgG2b was used as isotype control Ab for setting thresholds for positive staining. Numbers within histograms represent percentage of class II^+ glia; numbers in brackets depict MFI of the class II^+ population. Plots are representative of 3–4 experiments.

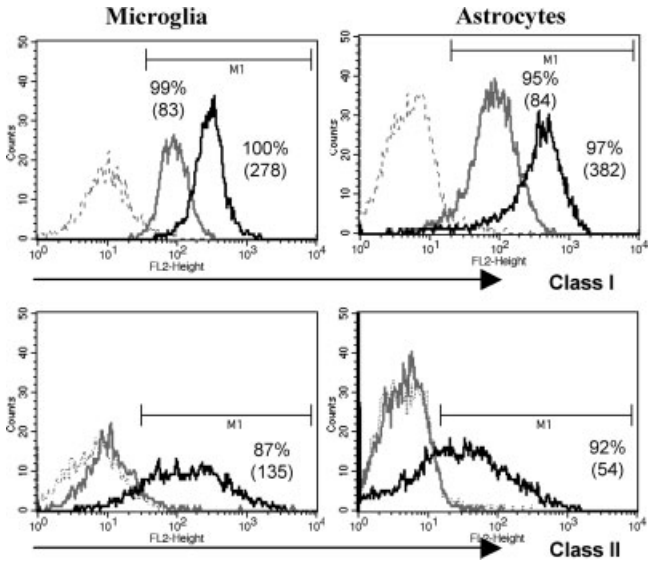

Fig. 6. MHC class I and class II expression on IFN-γ treated astrocytes. Mixed glial cultures from neonatal FVB/N mice were analyzed for CD45 and class I (top panel) and class II (bottom panel) expression after treatment with or without 1 ng/mL IFN-γ for 48 h. Cells were gated on microglia ($CD45^+$; left panel) or astrocytes ($CD45^-$; right panel). Microglia comprised ~30% of the culture. Microglia MHC expression on untreated cells is indicated by solid gray lines and on IFN-γ treated cells by solid black lines. Mouse IgG2a and Rat IgG2b, respectively, were used as isotype control Ab (dashed lines); control staining overlaps in untreated and treated cells. Numbers within histograms represent percentage of MHC^+ glia to the right (IFN-γ treated) or above (untreated) the respective population; numbers in brackets reveal MFI in the MHC^+ population.

strains (Aloisi et al., 2000; Dong and Benveniste, 2001; Hindinger et al., 2005; Stuve et al., 2002), MHC expression was also examined on microglia and astrocytes within mixed glial cultures prepared from neonatal FVB/N mice. Consistent with numerous previous reports, MHC class I was constitutively expressed on cultured astrocytes and microglia and the level of expression was increased in both cell types by IFN-γ treatment (see Fig. 6). The descrepency of constitutive class I expression may reside in prolonged growth in culture or in the immature nature of these glia compared with those derived and analyzed *ex vivo* from adult mice. MHC class II was below the level of detection in untreated cultures, but up-regulated by IFN-γ on both microglia and astrocytes, although upregulation was more tentative on astrocytes (see Fig. 6). Thus, no strain dependent alterations in MHC expression were detected on the GFP^+ astrocytes derived from the transgene expressing FVB/N mice.

IFN-γ In the CNS

Initial up-regulation of MHC molecules by day 5 p.i. coincides with infiltration of NK cells, $CD8^+$, and $CD4^+$ T cells, all potential sources of IFN-γ. IFN-γ is a potent antiviral cytokine that also enhances MHC class I and class II expression on microglia during JHMV infection (Bergmann et al., 2003). IFN-γ protein levels were thus measured at 3–17 days p.i. to directly gauge IFN-γ secretion in the inflamed CNS. No IFN-γ was detected at day 3 p.i. IFN-γ peaked rapidly between days 5 and 7 p.i. and the levels declined dramatically by day 10 p.i. (see Fig. 7). Overall, IFN-γ levels detected within the CNS coincided

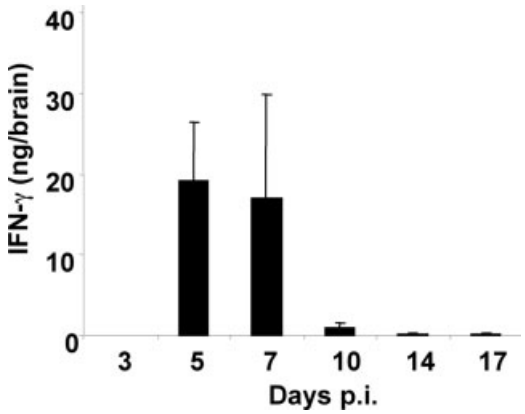

Fig. 7. IFN-γ in the CNS of FVB/N mice following virus infection. IFN-γ protein was measured by capture ELISA in cell free supernatants derived from homogenized brain preparations at the indicated times p.i. Data are representative of 2 separate experiments containing samples from 4 individual mice each per time point.

with the robust up-regulation of class I on astrocytes (Fig. 4A) and class II on microglia at day 5 p.i. (Fig. 5A). The high level of IFN-γ present at day 5 p.i. suggests that NK and T cells secreted abundant IFN-γ per cell, as T cell numbers were comparable to NK cell numbers at day 5 p.i., but significantly lower than T cells at day 7 p.i. Although a contribution by NK cells cannot be ruled out, the high virus antigen load, in addition to robust MHC molecule surface expression at day 5 p.i., supports the concept that MHC molecule-TCR interactions are responsible for IFN-γ release (Slifka et al., 1999; Liu and Whitton, 2005). Similarly, the abrupt decline in IFN-γ at day 10 p.i., coincident with the control of virus replication, may reflect limited TCR engagement by MHC molecules presenting viral antigen, despite sustained MHC expression. Alternatively, upregulation of inhibitory ligands may block sustained IFN-γ expression (Barber et al., 2006; Suvas et al., 2006).

DISCUSSION

The contribution of astrocytes to antigen presentation during inflammatory responses in the adult CNS is controversial. Although both MHC class I and class II molecule expression is readily induced in astrocytes cultured from neonates, MHC surface expression on astrocytes in the inflamed CNS has been difficult to confirm in adults. In the present study a neurotropic coronavirus infection was used to induce CNS inflammation in mice expressing GFP under the GFAP promoter, thus facilitating analysis of astrocytes by flow cytometry. The virus variant used replicates prominently in microglia/macrophages, astrocytes and oligodendrocytes, but rarely in neurons, and induces a lymphocyte dependent sublethal demyelinating disease (Bergmann et al., 2006). Whereas MHC class I up-regulation was readily demonstrable on astrocytes following infection, class II expression was tentative at best, despite strong expression on microglia. Delayed up-regulation of MHC class I on astrocytes compared with microglia further suggested that expression by astrocytes is more constrained compared with microglia. Early class I up-regulation on microglia following virus infection is consistent with IFN-γ independent induction (Bergmann et al., 2003) and is likely mediated by virus induced type I interferons (Rempel et al., 2004; Zhou et al., 2005). The apparent delay of astrocytes to up-regulate class I expression *in vivo* may be due to an inherent unresponsiveness to IFNα/β; however, virus infection itself and type I interferons enhance class I expression on cultured, neonatal astrocytes (Kraus et al., 1992; Massa et al., 1986). The robust up-regulation of class I on astrocytes and both class I and class II on microglia coincident with maximal IFN-γ detection implicates IFN-γ as a driving force for antigen presentation. T cells are the most likely source of IFN-γ, as the absence of NK cells does not alter MHC molecule expression patterns following JHMV infection in C56BL/6 mice (Zuo et al., 2006). The increased CNS infiltration of $CD4^+$ T cells, compared with $CD8^+$ T cells, in response to JHMV infection is unique to infected FVB/N mice and suggests that $CD4^+$ T cells may make a prominent contribution to IFN-γ secretion in the local environment. However, neither class I or class II restricted viral epitopes have been mapped in this haplotype, preempting experimental verification.

Class I expression on astrocytes is consistent with a perforin mediated mechanism of viral clearance from this cell type (Bergmann et al. 2003; Lin et al., 1997; Parra et al., 1999) and the capacity of astrocytes to perpetuate class I restricted $CD8^+$ T cells (Sedgwick et al., 1991). Interactions of class I expressing astrocytes with $CD8^+$ T cells *in vivo* are further supported by selective destruction of a subset of the astrocytes expressing a neo-autoantigen following transfer of autoantigen specific TCR transgenic $CD8^+$ T cells (Cabarrocas et al., 2003) and by immunological synapse formation between virally infected astrocytes and $CD8^+$ T cells (Barcia et al., 2006). The inability to detect class I on astrocytes following infection with a related neurotropic JHMV variant, which infects both neurons and glial cells may reside in limitations imposed by histological analysis, although class I is detected on oligodendrocytes, microglia, and neurons (Redwine et al., 2001). Therefore, the difference in astrocyte responsiveness may also reflect a unique cytokine milieu induced by each virus. Neurotropic coronavirus variants induce both differential kinetics and magnitude of type I and type II IFN mRNA (Parra et al., 1997; Remple et al., 2004), which may affect class I heavy chains as well as the genes involved in antigen processing and presentation (Strehl et al., 2005). The kinetics of class I and class II up-regulation on microglia in JHMV infected FVB/N mice used in this study are similar to those in BALB/c and C57BL/6 mice (Bergmann et al., 2003; Zuo et al., 2006) suggesting different genetic backgrounds do not suffice to explain these contradictory results.

The apparent impairment in astrocytes to express class II molecules during acute viral encephalomyelitis, despite the presence of abundant IFN-γ, is reminiscent of the

inability to detect class II in this cell type by immunohistological analysis (Horwitz et al., 1999; Redwine et al., 2001). Similarly, class II expression was essentially absent from astrocytes in EAE lesions of wt mice (Stuve et al., 2002). CIITA is essential for class II gene transcription in astrocytes (LeibundGut-Landmann et al., 2004; Waldburger et al., 2001). However, although transgene driven constitutive CIITA results in class II expression on astrocytes in non-inflamed CNS tissue, only a very limited number of class II expressing astrocytes are present in EAE lesions in these mice (Stuve et al., 2002). Similarly, although class II positive astrocytes have been detected in lesions during relapsing EAE (Sakai et al., 1986), the paucity of class II up-regulation on astrocytes compared with microglia, demonstrates *in vivo* cell type specific regulation. These data support that CIITA expression is selectively suppressed in astrocytes during acute inflammation, even in the presence of IFN-γ. Transcriptional silencing may be due to epigenetic regulation or active suppression (Gresser et al., 2000; Landmann et al., 2001; Massa, 1993; Tooze et al., 2006). CIITA is regulated by numerous factors including IFN-γ, TGF-β, IL-1, IL-4, and IL-10 (Dong and Benveniste, 2001; LeibundGut-Landman et al., 2004; Rohn et al., 1996). While ineffective IFN-γ signaling by astrocytes cannot be excluded, prominent, yet delayed, class I expression suggests this pathway is intact. Furthermore, JHMV inflammation primarily constitutes a Th1-type response, as indicated by high IFN-γ protein levels and low IL-4 and IL-10 gene transcription (Parra et al., 1997) negating a role for anti-inflammatory cytokines. *In vitro*, other mediators inhibiting class II expression on astrocytes include TGF-β, IL-1β, IFN-β, glutamate, vasoactive intestinal peptide, norepinephrine, nitric oxide, and direct contact with neurons (Dong et al., 2001). An interesting candidate may be IFN-β which is rapidly induced following JHMV infection (Zhou et al., 2005), and acts downstream of CIITA transcription to block class II expression (Lu et al., 1995).

In summary the data demonstrate MHC class I up-regulation, and the absence of detectable class II expression, on the vast majority of astrocytes during virus induced inflammation. More stringent class I regulation by astrocytes, compared with microglia, may reside in reduced type I IFN and/or IFN-γ responsiveness or additional factors known to enhance IFN-γ mediated effects such as TNF-α. Although class I and class II expression correlate with IFN-γ levels, maintenance of class I surface expression on astrocytes and microglia, even after clearance of infectious virus, suggest that abrogation of IFN-γ secretion does not lead to immediate MHC molecule down regulation. Similarly, sustained class II expression on microglia suggests a low turnover rate of MHC molecules. Sustained MHC expression may provide an opportunity to activate autoantigen specific T cells. The expression of GFP in astrocytes enables future enrichment of this cell type for comparative gene profiling and additional insights into the regulation of antigen presentation by both distinct glial subsets and at distinct stages of inflammation.

ACKNOWLEDGMENTS

Authors thank Emanuel Dimacali and the USC Norris Cancer Center Flow Cytometry Core for assistance with flow cytometry. Authors also thank Wen Wei and Ernesto Baron for assistance with the histopathology and Eva Boruka for maintenance of the homozygous FVB/N-Tg[GFAPGFP]14Mes/J colony.

REFERENCES

Aloisi F, Serafini B, Adorini L. 2000. Glia-T cell dialogue. J Neuroimmunol 107:111–117.

Barber DL, Wherry EJ, Masopust D, Zhu B, Allison JP, Sharpe AH, Freeman GJ, Ahmed R. 2006. Restoring function in exhausted CD8 T cells during chronic viral infection. Nature 439:682–687.

Barcia C, Thomas CE, Curtin JF, King GD, Wawrowsky K, Candolfi M, Xiong WD, Liu C, Kroeger K, Boyer O, Kupiec-Weglinski J, Klatzmann D, Castro MG, Lowenstein PR. 2006. In vivo mature immunological synapses forming SMACs mediate clearance of virally infected astrocytes from the brain. J Exp Med 203:2095–2107.

Bergmann CC, Altman JD, Hinton D, Stohlman SA. 1999. Inverted immunodominance and impaired cytolytic function of $CD8^+$ T cells during viral persistence in the central nervous system. J Immunol 163:3379–3387.

Bergmann CC, Lane TE, Stohlman SA. 2006. Coronavirus infection of the CNS: Host-virus standoff. Nat Rev Microbiol 4:121–132.

Bergmann CC, Parra B, Hinton DR, Chandran R, Morrison M, Stohlman SA. 2003. Perforin-mediated effector function within the central nervous system requires IFN-γ-mediated MHC up-regulation. J Immunol 170:3204–3213.

Cabarrocas J, Bauer J, Piaggio E, Liblau L, Lassman H. 2003. Effective and selective immune surveillance of the brain by MHC class I-restricted cytotoxic T lymphocytes. Eur J Immunol 33:1174–1182.

Dong Y, Benveniste EN. 2001. Immune function of astrocytes. Glia 36:180–190.

Fierz W, Endler B, Reske K, Wekerle H, Fontana A. 1985. Astrocytes as antigen-presenting cells. I. Induction of Ia antigen expression on astrocytes by T cells via immune interferon and its effect on antigen presentation. J Immunol 134:3785–3793.

Fleming JO, Trousdale MD, el-Zaatari FA, Stohlman SA, Weiner LP. 1986. Pathogenicity of antigenic variants of murine coronavirus JHM selected with monoclonal antibodies. J Virol 58:869–875.

Gilmore W, Correale J, Weiner LP. 1994. Coronavirus induction of class I major histocompatibility complex expression in murine astrocytes is virus strain specific. J Exp Med 180:1013–1023.

Gonzalez JM, Bergmann CC, Fuss B, Hinton DR, Kangas C, Macklin WB, Stohlman SA. 2005. Expression of a dominant negative IFN-γ receptor on mouse oligodendrocytes. Glia 51:22–34.

Gresser O, Hein A, Riese S, Regnier-Vigouroux A. 2000. Tumor necrosis factor α and interleukin-1 α inhibit through different pathways interferon-γ-induced antigen presentation, processing and MHC class II surface expression on astrocytes, but not on microglia. Cell Tissue Res 300:373–382.

Hickey WF. 2001. Basic principles of immunological surveillance of the normal central nervous system. Glia 36:118–128.

Hindinger C, Gonzalez J, Bergmann CC, Fuss B, Hinton DR, Atkinson R, Macklin W, Stohlman SA. 2005. Astrocyte expression of a dominant-negative IFN-γ receptor. J Neurosci Res 82:20–31.

Horwitz MS, Evans CF, Klier FG, Oldstone MB. 1999. Detailed in vivo analysis of interferon-γ induced major histocompatibility complex expression in the the central nervous system: Astrocytes fail to express major histocompatibility complex class I, II molecules. Lab Invest 79:235–242.

Kraus E, Schneider-Schaulies S, Miyasaka M, Tamatani T, Sedgwick J. 1992. Augmentation of major histocompatibility complex class I, ICAM-1 expression on glial cells following measles virus infection: Evidence for the role of type-1 interferon. Eur J Immunol 22:175–82.

Lampson LA. 1995. Interpreting MHC class I expression and class I/class II reciprocity in the CNS: Reconciling divergent findings. Microsc Res Tech 32:267–285.

Landmann S, Muhlethaler-Mottet A, Bernasconi L, Suter T, Waldburger JM, Masternak K, Arrighi JF, Hauser C, Fontana A, Reith W. 2001. Maturation of dendritic cells is accompanied by rapid transcriptional silencing of class II transactivator (CIITA) expression. J Exp Med 194:379–391.

Lavi E, Gilden DH, Highkin MK, Weiss SR. 1984. Persistence of mouse hepatitis virus A59 RNA in a slow virus demyelinating infection in mice as detected by in situ hybridization. J Virol 51:563–566.

Lavi E, Suzumura A, Murray EM, Silberberg DH, Weiss S. 1989. Induction of MHC class I antigens on glial cells is dependent on persistent mouse hepatitis virus infection. J Neuroimmunol 22:107–111.

LeibundGut-Landmann S, Waldburger JM, Krawczyk M, Otten LA, Suter T, Fontana A, Acha-Orbea H, Reith W. 2004. Mini-review: Specificity and expression of CIITA, the master regulator of MHC class II genes. Eur J Immunol 34:1513–1525.

Lin MT, Stohlman SA, Hinton DR. 1997. Mouse hepatitis virus is cleared from the central nervous systems of mice lacking perforin-mediated cytolysis. J Virol 71:383–391.

Liu F, Whitton JL. 2005. Cutting edge: Re-evaluating the in vivo cytokine responses of $CD8^+$ T cells during primary and secondary viral infections. J Immunol 174:5936–5940.

Lu HT, Riley JL, Babcock GT, Huston M, Stark GR, Boss JM, Ransohoff RM. 1995. Interferon (IFN) β acts downstream of IFN-γ-induced class II transactivator messenger RNA accumulation to block major histocompatibility complex class II gene expression and requires the 48-kD DNA-binding protein, ISGF3-γ. J Exp Med 182:1517–1525.

Massa PT. 1993. Specific suppression of major histocompatibility complex class I, class II genes in astrocytes by brain-enriched gangliosides. J Exp Med 178:1357–1363.

Massa PT, Dorries R, ter Meulen V. 1986. Viral particles induce Ia antigen expression on astrocytes. Nature 320:543–546.

Massa PT, Ozato K, McFarlin DE. 1993. Cell type-specific regulation of major histocompatibility complex (MHC) class I gene expression in astrocytes, oligodendrocytes, and neurons. Glia 8:201–207.

Momburg F, Koch N, Moller P, Moldenhauer G, Butcher GW, Hammerling GJ. 1986. Differential expression of Ia and Ia-associated invariant chain in mouse tissues after in vivo treatment with IFN-γ. J Immunol 136:940–948.

Parra B, Hinton DR, Lin MT, Cua DJ, Stohlman SA. 1997. Kinetics of cytokine mRNA expression in the CNS following lethal and sublethal coronavirus-induced encephalomyelitis. Virology 233:260–270.

Parra B, Hinton DR, Marten NW, Bergmann CC, Lin MT, Yang CS, Stohlman SA. 1999. IFN-γ is required for viral clearance from central nervous system oligodendroglia. J Immunol 162:1641–1647.

Perlman S, Ries D. 1987. The astrocyte is a target cell in mice persistently infected with mouse hepatitis virus, strain JHM. Microb Pathog 3:309–314.

Ramakrishna C, Atkinson R, Stohlman S, Bergmann C. 2006. Vaccine induced memory $CD8^+$ T cells cannot prevent virus reactivation. J Immunol 176:3062–3069.

Ramakrishna C, Bergmann CC, Atkinson R, Stohlman SA. 2003. Control of central nervous system viral persistence by neutralizing antibody. J Virol 77:4670–4678.

Ramakrishna C, Stohlman SA, Atkinson RD, Shlomchik MJ, Bergmann CC. 2002. Mechanisms of central nervous system viral persistence: The critical role of antibody and B cells. J Immunol 168:1204–1211.

Redwine JM, Buchmeier MJ, Evans CF. 2001. In vivo expression of major histocompatibility complex molecules on oligodendrocytes and neurons during viral infection. Am J Pathol 159:1219–1224.

Rempel JD, Murray SL, Meisner J, Buchmeier MJ. 2004. Differential regulation of innate and adaptive immune responses in viral encephalitis. Virology 318:381–392.

Rohn WM, Lee YJ, Benveniste EN. 1996. Regulation of class II MHC expression. Crit Rev Immunol 16:311–330.

Sakai K, Tabira T, Endoh M, Steinman L. 1986. Ia expression in chronic relapsing experimental allergic encephalomyelitis induced by long-term cultured T cell lines in mice. Lab Invest 54:345–52.

Sedgwick JD, Hickey W. 1997. Antigen presentation in the central nervous system. In: Keane RW, Hickey WF, editors. Immunology of the central nervous system. Oxford: Oxford University Press. p 364.

Sedgwick JD, Mossner R, Schwender S, ter Meulen V. 1991. Major histocompatibility complex-expressing nonhematopoietic astroglial cells prime only $CD8^+$ T lymphocytes: Astroglial cells as perpetuators but not initiators of $CD4^+$ T cell responses in the central nervous system. J Exp Med 173:1235–1246.

Slifka MK, Rodriguez F, Whitton JL. 1999. Rapid on/off cycling of cytokine production by virus-specific $CD8^+$ T cells. Nature 401:76–79.

Strehl B, Seifert U, Kruger E, Heink S, Kuckelkorn U, Kloetzel PM. 2005. Interferon-γ, the functional plasticity of the ubiquitin-proteasome system, and MHC class I antigen processing. Immunol Rev 207:19–30.

Stuve O, Youssef S, Slavin AJ, King CL, Patarroyo JC, Hirschberg DL, Brickey WJ, Soos JM, Piskurich JF, Chapman HA, Zamvil SS. 2002. The role of the MHC class II transactivator in class II expression and antigen presentation by astrocytes and in susceptibility to central nervous system autoimmune disease. J Immunol 169:6720–6732.

Suvas S, Azkur AK, Rouse BT. 2006. Qa-1b and CD94-NKG2a interaction regulate cytolytic activity of herpes simplex virus-specific memory $CD8^+$ T cells in the latently infected trigeminal ganglia. J Immunol 176:1703–11.

Suzumura A, Lavi E, Weiss SR, Silberberg DH. 1986. Coronavirus infection induces H-2 antigen expression on oligodendrocytes and astrocytes. Science 232:991–993.

Tooze RM, Stephenson S, Doody GM. 2006. Repression of IFN-γ induction of class II transactivator: A role for PRDM1/Blimp-1 in regulation of cytokine signaling. J Immunol 177:4584–93.

Traugott U, Scheinberg LC, Raine CS. 1985. On the presence of Ia-positive endothelial cells and astrocytes in multiple sclerosis lesions and its relevance to antigen presentation. J Neuroimmunol 8:1–14.

Waldburger JM, Suter T, Fontana A, Acha-Orbea H, Reith W. 2001. Selective abrogation of major histocompatibility complex class II expression on extrahematopoietic cells in mice lacking promoter IV of the class II transactivator gene. J Exp Med 194:393–406.

Wang FI, Hinton DR, Gilmore W, Trousdale MD, Fleming JO. 1992. Sequential infection of glial cells by the murine hepatitis virus JHM strain (MHV-4) leads to a characteristic distribution of demyelination. Lab Invest 66:744–754.

Wong GH, Bartlett PF, Clark-Lewis I, Battye F, Schrader JW. 1984. Inducible expression of H-2 and Ia antigens on brain cells. Nature 310:688–691.

Wong GH, Bartlett PF, Clark-Lewis I, McKimm-Breschkin JL, Schrader JW. 1985. Interferon-γ induces the expression of H-2 and Ia antigens on brain cells. J Neuroimmunol 7:255–278.

Xiao BG, Link H. 1998. Immune regulation within the central nervous system. J Neurol Sci 157:1–12.

Zhou J, Marten N, Bergmann CC, Macklin W, Hinton DR, Stohlman SA. 2005. Expression of matrixmetalloproteinases and their tissue inhibitor during viral encephalitis. J Virol 79:4764–4773.

Zhuo L, Sun B, Zhang CL, Fine A, Chiu SY, Messing A,. 1997. Live astrocytes visualized by green fluorescent protein in transgenic mice. Dev Biol 187:36–42.

Zuo J, Stohlman SA, Hoskin J, Hinton D, Atkinson R, Bergmann C. 2006. Mouse hepatitis virus pathogenesis in the central nervous system is independent of IL-15 and natural killer cells. Virology 350:206–215.